



## OPEN ACCESS

## EDITED BY

Markus Meier,  
Leibniz Institute for Baltic Sea Research (LG),  
Germany

## REVIEWED BY

Jian Su,  
Danish Meteorological Institute (DMI), Denmark  
Lidia Gaslikova,  
Helmholtz Centre for Materials and Coastal  
Research (HZG), Germany

## \*CORRESPONDENCE

Nils H. Schade,  
✉ nils.schade@bsh.de

RECEIVED 28 March 2025

ACCEPTED 13 June 2025

PUBLISHED 08 July 2025

## CITATION

Schade NH, Jensen C and Kruschke T (2025)  
Large scale atmospheric conditions favoring  
storm surges in the North and Baltic Seas and  
possible future changes.  
*Front. Environ. Sci.* 13:1601836.  
doi: 10.3389/fenvs.2025.1601836

## COPYRIGHT

© 2025 Schade, Jensen and Kruschke. This is an  
open-access article distributed under the terms  
of the [Creative Commons Attribution License](#)  
(CC BY). The use, distribution or reproduction in  
other forums is permitted, provided the original  
author(s) and the copyright owner(s) are  
credited and that the original publication in this  
journal is cited, in accordance with accepted  
academic practice. No use, distribution or  
reproduction is permitted which does not  
comply with these terms.

# Large scale atmospheric conditions favoring storm surges in the North and Baltic Seas and possible future changes

Nils H. Schade\*, Corinna Jensen and Tim Kruschke

Federal Maritime and Hydrographic Agency (BSH), Hamburg, Germany

Climate change will not only cause significant sea level rise but is likely to also change the large-scale atmospheric circulation. Here, we analyse atmospheric conditions that caused storm surges at the German North and Baltic Sea coasts. Possible future changes thereof are examined using a multi-model CMIP6 ensemble of global climate simulations under different emission scenarios. Observed storm surges are analyzed from peak water level observations at the gauge stations Koserow, Warnemünde, Kiel-Holtenau, and Flensburg along the German Baltic Sea coast, and at Cuxhaven located in the North Sea. For the classification of the meteorological conditions on the respective day of a storm surge we use two atmospheric reanalyses. We employ a simple weather type classification approach, based on daily mean sea-level pressure fields as input. This approach can be applied easily to global or regional climate model simulations which makes it an effective tool for climate change investigations. For each of the gauge stations, a proxy for storm surge favorable atmospheric conditions—the effective wind—is derived. Westerly and cyclonic weather types are the atmospheric drivers of observed storm surges at Cuxhaven. The most favorable weather types at the stations Koserow and Warnemünde are north-east and cyclonic, adding anticyclonic for Kiel-Holtenau and Flensburg. Towards the end of the 21st century, the CMIP6 ensemble projects a significant increase in the frequency of westerly effective winds for Cuxhaven under the scenarios SSP3-7.0 and SSP5-8.5. In contrast, a significant decrease of easterly effective winds is projected for all four locations at the Baltic Sea coast. These findings are a result of the tendency towards strengthened westerly stream and a north-western shift of the storm tracks in climate projections over these regions that is also described by other investigations. Our results indicate that the increasing risk for extreme water levels associated with the virtually certain sea-level rise is additionally fueled by more frequent weather patterns favoring storm surges at the German North Sea coast, while changes of the large-scale circulation may dampen the increase of storm surge risk associated with sea-level rise at the German Baltic Sea coast to some degree.

## KEYWORDS

storm surges, weather types, gales, wind, North Sea, Baltic Sea, CMIP6, climate change

# 1 Introduction

Storm surges cause a significant rise in coastal water levels that can have significant socio-economic consequences and—in extreme cases—may even result in fatalities. Furthermore, these extreme water levels (EWLs), in combination with strong winds and long-lasting precipitation events, can severely impact on- and offshore transport system and its infrastructure (e.g., [Buthe et al., 2015](#); [Kew et al., 2013](#); [Schade, 2017](#)). Disruptions to transport and traffic chains may lead to delays, re-routing, and thus secondary financial consequences and maybe even additional human losses not only at the direct coastline but also far inland.

In this study, we investigate the large-scale atmospheric conditions associated with storm surges along the German North and Baltic Seas coastlines, as well as their projected changes under future climate scenarios. The goal is to support the assessment of potential implications on off- and onshore transport systems. To characterize the large scale circulation, we employ a weather type classification method originally developed by [Lamb \(1950\)](#) which is used operationally at the German Federal Maritime and Hydrographic Agency (BSH). This method is applied to atmospheric reanalyses for the recent past (1971–2000) and climate model projections for the far future (2071–2100).

Our study builds on previous research examining the representation and potential changes in atmospheric circulation and wind speeds over Central Europe. [Herrera-Lormendez et al. \(2022\)](#) for example, show that the weather type classification method by [Jenkinson and Collison \(1977\)](#) applied over Germany reproduced the occurrence of the observed circulation patterns, as well as the interannual variability and its climatological frequencies. Several climate change studies show a poleward shift of the storm tracks over Europe in a warming climate with an increase in westerly conditions ([Barnes and Polvani, 2013](#); [Bengtsson et al., 2006](#); [Harvey et al., 2020](#); [Mbengue and Schneider, 2013](#); [Priestley et al., 2020](#); [Wu et al., 2011](#)). These tendencies are visible in global climate models (GCMs; e.g., [Donat et al., 2010](#)) as well as in high resolution regional models (RCMs; e.g., [Plavcová and Kyselý, 2013](#)). The increase in westerly conditions is accompanied by a profound decrease of easterly conditions during the winter months. Both signals are robust in both the global ([Demuzere et al., 2009](#); [Stryhal and Huth, 2019](#)) and the regional ([Riediger and Gratzki, 2014](#)) simulations. Furthermore, an increase in westerly conditions would lead to an increase in the occurrence of resulting storm surges at the German North Sea coast while a decrease in easterly conditions would lead to a decrease of resulting storm surges at the German Baltic Sea coast due to their exposure to the respective direction.

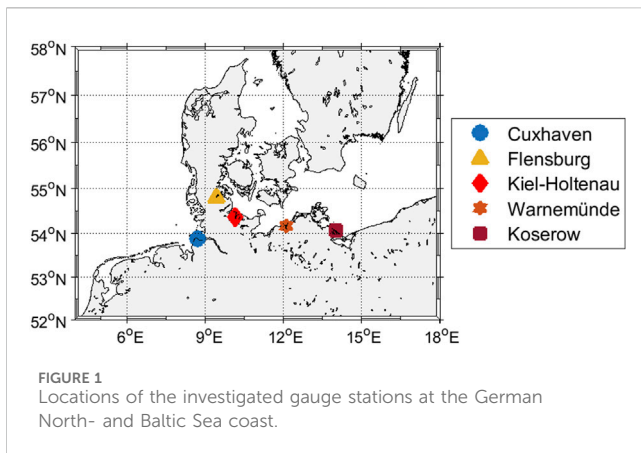
However, comparisons of historical storm surges with climate projections based on RCP (Representative Concentration Pathways) scenarios of a small regional ensemble in the North Sea area did not show significant changes in extreme wind speeds until 2,100 ([Bott et al., 2020](#)). At most, a slightly positive trend could be seen in the south-eastern North Sea, as well as a small increase in the occurrence of westerly winds. These trends were always within the yearly and decadal variability of the respective models and, therefore, not robust. Other studies employed a different method and identified single low-pressure systems and their paths. In a recent investigation [Meyer and Gaslikova \(2024\)](#) used an atmospheric reanalysis driven

tide surge model to simulate water levels during severe storm tides - a storm tide consists of the normal astronomical tide plus the storm surge caused by the atmospheric conditions - over the last 120 years in the German Bight.

Europe lies at the “Exit” of the North Atlantic storm tracks, where, climatologically, there is a local maximum in the passage of intensified low-pressure systems. Many climate models project a future increase in both the frequency and the intensity of storms affecting the British Island, the North Sea and northern Central Europe ([Donat et al., 2010](#); [Zappa and Shepherd, 2017](#)). However, it is apparent that different models yield varying and sometimes even contradictory results. This uncertainty leads to the necessity to conduct climate change analyses on the basis of an ensemble of models of sufficient size and quality, as done within the sixth assessment report of the Intergovernmental Panel on Climate Change (IPCC; Intergovernmental Panel on Climate Change (IPCC), 2022).

Investigations of the latest CMIP6 model generation have shown notable improvements over previous generations, not only in terms of higher model resolution but also in the representation of model physics. They can reproduce the northern hemispherical storm tracks better and show smaller deviations compared to reanalyses ([Harvey et al., 2020](#); [Priestley et al., 2020](#)). A recent study also shows the usability of the Hess and Brezowsky “Großwetterlagen” ([Hess and Brezowsky, 1952](#)) using a deep learning ensemble for automatic classification of weather types for an ensemble of 31 CMIP6 climate model simulations. [Heinrich et al. \(2024\)](#) found a robust increase in the frequency of the atmospheric pattern Cyclonic Westerly towards the end of the 21st century during the winter months among all models and scenarios. This pattern is associated with compound flooding events, caused by a combination of strong (but not necessarily extreme) or long-lasting precipitation, on-shore winds, and high water levels at the European Coasts.

Our study complements the research by [Jensen et al. \(2022\)](#) investigating the opposing extreme, the so called “negative storm surges”: The large ensemble produced by the Swedish Meteorological and Hydrological Institute (SMHI-LENS; [Wyser et al., 2021](#)), employing the atmosphere-ocean general circulation model EC-Earth3 ([Döscher et al., 2022](#)) was used to robustly isolate the climate change signal from the background of internal variability by comprising 50 simulations for each, the historical period 1970–2014 and different scenarios covering the period 2015–2100. In our study we use an ensemble of different runs from different CMIP6 models to improve the robustness of possible climate change signals regarding storm surges. Further, this approach has two distinct advantages: (i) the substantial model uncertainty of climate change signals related to extra-tropical cyclones and associated wind storms demands for large multi-model ensembles to allow for a robust assessment of any potential climate change signal in this respect; (ii) despite not being perfect, global climate models with given resolution are arguably better in representing the sea level pressure pattern of extra-tropical cyclones than all types of meso-scale wind fields associated with the frontal systems of the storms. Hence, our rather simple approach should be less affected by existing model deficiencies than any analysis of the model wind speeds themselves (see e.g., [Krieger and Weisse, 2025](#)). In addition, some recent studies have already shown that the CMIP6 models outperform the older



model generations in the representation of the atmospheric circulation over Europe based on the same objective classification method we use in this study (e.g., Brands, 2022; Fernandez-Granja et al., 2021).

In the following we first introduce the data and methods used in this study (Section 2). We assign observed storm peak water levels at four stations in the Baltic Sea and one in the North Sea to weather types derived from ERA5 and NCEP sea level pressure data and identify atmospheric situations favouring storm surges at the respective tide gauges. Then, we investigate possible future changes of these situations using a CMIP 6 GCM ensemble (Section 3). Finally, we discuss our findings (Section 4).

## 2 Data and methods

### 2.1 Data

#### 2.1.1 Observational water level data from gauge stations

We use observations of the storm peak water levels at the gauges in Flensburg, Kiel-Holtenau, Warnemünde, and Koserow located at the German Baltic Sea Coast, as well as in Cuxhaven in the German Bight of the North Sea (see Figure 1) for the period 1951–2022. Water levels for Cuxhaven have been downloaded from the Portal Zentrales Datenmanagement (ZDM) Küstendaten of the German Federal Waterways and Shipping Administration (WSV, last access 25 June 2022)<sup>1</sup>. Water levels for the Baltic Sea stations have been provided by the BSH (personal communication, Ines Perlet-Markus and Jürgen Holfort).

#### 2.1.2 Atmospheric reanalysis data

For the analysis of past meteorological conditions associated with the observed storm surges, we use both the NCEP/NCAR R1 and the ERA5 reanalyses sea level pressure (SLP) data.

The National Centers for Environmental Prediction (NCEP) and the National Center for Atmospheric Research (NCAR) produced the Reanalysis 1 (Kalnay et al., 1996) in close cooperation. The central module is identical to the operational system then used at the NCEP, but with a spectral T62 horizontal resolution, i.e., about 210 km grid spacing and 28 vertical levels. The reanalysis was initially completed in 1996, but continued through an identical Climate Data Assimilation System (CDAS) to ensure consistency with the earlier decades.

ERA5 is one of the most recent reanalysis datasets produced by the European Centre for Medium-Range Weather Forecasts (ECMWF, Hersbach et al., 2020). As such, it is one of the most modern and advanced global reanalyses, using the Integrated Forecasting System (IFS) jointly developed and maintained by ECMWF and Météo-France. The ERA5 data are available on a high-resolution grid with a spacing of 0.25° and in hourly resolution for the period from 1979 to the present and are updated at regular intervals. To additionally cover the period before 1978 we included the ERA5 backward extension (Bell et al., 2021). For this investigation we calculated daily means of the hourly SLP values from 0UTC to 23UTC. The daily SLP means are used to calculate daily weather type classifications, Gale strengths and effective winds.

#### 2.1.3 Climate model simulations

In order to analyse the potential future change of meteorological conditions favorable for storm surges at the German coasts, we make use of an ensemble of global climate models. All simulations of a given experiment are subject to identical external forcings, such as greenhouse gases and aerosols, following the protocol for the historical experiment of the Coupled Model Intercomparison Project in its sixth phase (CMIP6) (Eyring et al., 2016), and ScenarioMIP (O'Neill et al., 2016), respectively. For the analyses presented in this study, we examined the four Tier1-scenarios of ScenarioMIP that is SSP1-2.6, SSP2-4.5, SSP3-7.0, and SSP5-8.5. The SSP (Shared Socioeconomic Pathways) scenarios span a wide range of socioeconomic narratives and greenhouse gas concentration pathways for the remainder of the 21st century (Riahi et al., 2017).

The large number of simulations available for CMIP6 makes it an excellent tool to derive robust estimates of climate change signals projected by these models. Our analyses were based on daily mean SLP fields taken from these simulations. In order to be able to compare our results with a different method that has recently been successfully tested for past storm surges at Cuxhaven (Schaffer et al., 2024), we use only models with a high temporal resolution for the wind components in our ensemble. Altogether, our ensemble consists of seven different GCMs and in total 23 model runs (Table 1).

## 2.2 Methods

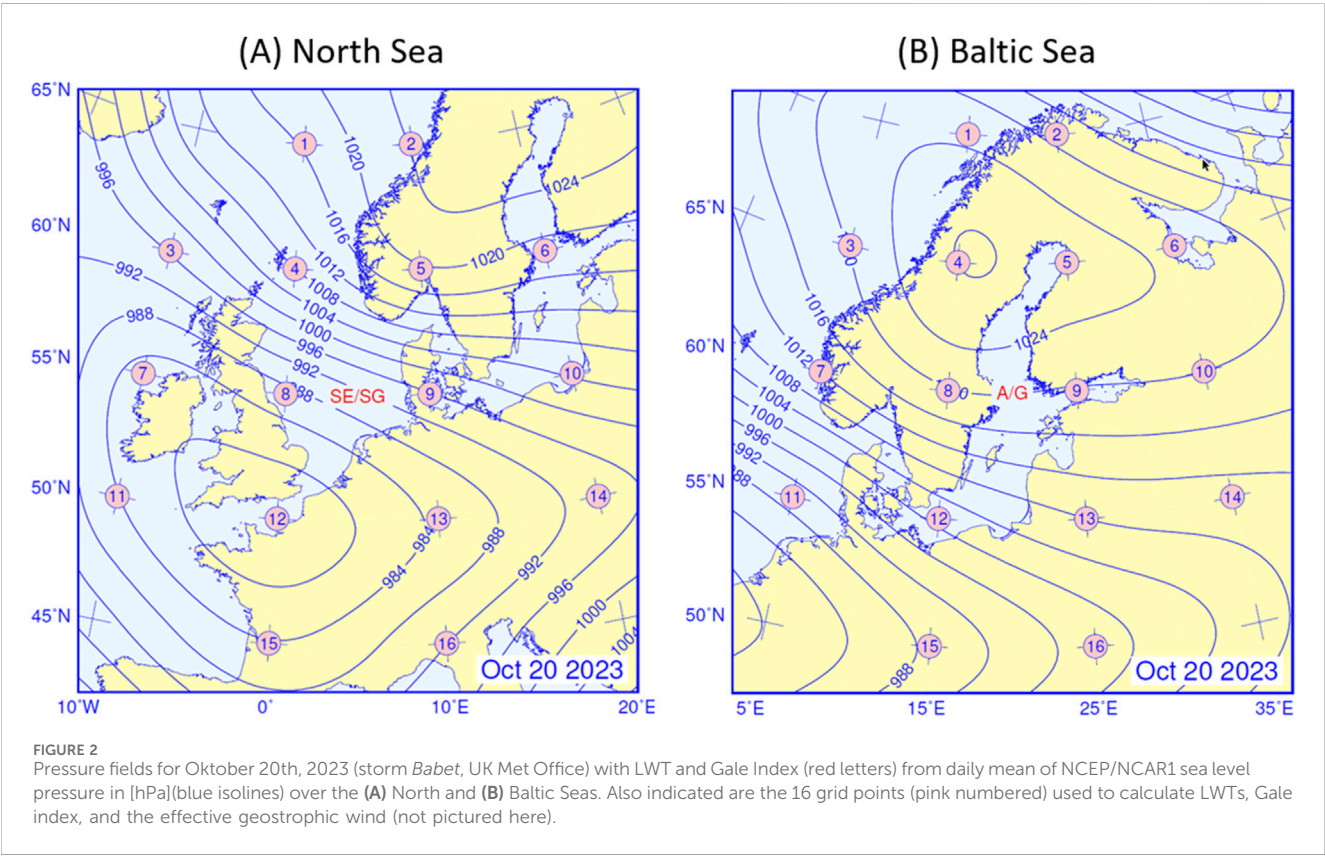
### 2.2.1 Defining storm surges

For the German North Sea coast, storm surges are defined as EWLs exceeding 1.5 m above the mean high water (Bundesamt für Seeschifffahrt, 2025). 272 storm tides and respective peak water levels were recorded at the gauge Cuxhaven in the period 1951–2022, which corresponds to an average of about four storm

<sup>1</sup> [https://www.c.de/DE/Services/Messreihen\\_Dateien\\_Download/Download\\_Zeitreihen\\_node.html](https://www.c.de/DE/Services/Messreihen_Dateien_Download/Download_Zeitreihen_node.html).

TABLE 1 Global climate models (GCMs) used for this investigation, including the resolution of the model components for the atmosphere und the ocean, references, scenarios and the respective runs.

GCM	Resolution	References	Scenario	Run
CMCC-CM2-SR5	Atmosphere: CAM5.3 (1 deg lat/lon)	Cherchi et al. (2018)	historical, ssp126, ssp245, ssp370, ssp585	r1i1p1f1
	Ocean: NEMO3.6 (1–0.33 deg lat/lon)			
CNRM-CM6-1-HR	Atmosphere: Arpege 6.3 (0.5 deg lat/lon)	Voldoire et al. (2019)	historical, ssp126, ssp245, ssp370, ssp585	r1i1p1f2
	Ocean: NEMO3.6 (0.25 deg lat/lon)			
EC-Earth3	Atmosphere: IFS cy36r4 (80 km lat/lon)	Döscher et al. (2022)	historical, ssp126, ssp245, ssp370, ssp585	r1i1p1f1
	Ocean: NEMO3.6 (1–0.33 deg lat/lon)			
IPSL-CM6A-LR	Atmosphere: LMDZ NPv6 (1 deg lat/lon)	Boucher et al. (2020)	historical, ssp126, ssp245, ssp370, ssp585	r1-r4i1p1f1 r6i1p1f1 r14i1p1f1
	Ocean: NEMO-OPA (1 deg lat/lon)			
MIROC6	Atmosphere: CCSR AGCM (150 km lat/lon)	Tatebe et al. (2019)	historical, ssp126, ssp245, ssp370, ssp585	r1i1p1f1 r2i1p1f1 r3i1p1f1
	Ocean: COCO4.9 (1 deg lat/lon)			
MPI-ESM1-2-LR	Atmosphere: ECHAM6.3 (200 km lat/lon)	Mauritsen et al. (2019)	historical, ssp126, ssp245, ssp370, ssp585	r1-r10i1p1f1
	Ocean: MPIOM1.63 (1.5 deg lat/lon)			
MRI-ESM2-0	Atmosphere: MRI-AGCM3.5 (120 km lat/lon)	Yukimoto et al. (2019)	historical, ssp126, ssp245, ssp370, ssp585	r1i1p1f1
	Ocean: MRI.COM4.4 (0.5–0.3 deg lat/lon)			



tides per year. It should be emphasized here that these events are not necessarily independent of each other. A large-scale synoptic weather situation may lead to a succession of several high waters that meet the criterion of a storm surge given here. In the following,

we detect and treat each storm tide as a separate event ignoring their possible dependence.

For the German Baltic Sea coast, storm surges are defined as EWLs exceeding 1 m above the mean water level (MWL). 184 storm



tides were recorded at the gauge Flensburg, 161 at the gauge Kiel-Holtenau, 103 at the gauge Warnemünde, and 105 at the gauge Koserow.

## 2.2.2 Classification of the large-scale atmospheric circulation

A coherent description of the large-scale atmospheric circulation is possible using defined circulation patterns or weather types (e.g., Lamb, 1950). At BSH, the automatic classification method developed by Jenkinson and Collison (Jenkinson and Collison, 1977) to objectify the “Lamb Weather Types” (hereafter LWTs) is used operationally as part of the analysis of the state of the North Sea region (Löwe, 2005), and, since 2020, for the Baltic Sea region as well. This classification method is also applied in this study. It is solely based on daily means of the SLP fields at 16 grid points  $p_x$  (with  $x = 1 \dots 16$ ) in the extended North or Baltic Sea region (see Figure 2) to calculate the vector components ( $u^*, v^*$ ) of the geostrophic wind ( $V^*$ ) and the vorticity ( $\zeta^*$ ) as described by Löwe (2005), appendix A, GL. A5 - A7 & GL. A13/14), where

$$V^* (hPa) = \sqrt{u^{*2} + v^{*2}}$$

with

$$u^* (hPa) = \frac{1}{2} (p_{12} + p_{13}) - \frac{1}{2} (p_4 + p_5)$$

$$v^* (hPa) = \frac{1}{\cos \varphi_0} \left\{ \frac{1}{4} (p_5 + 2p_9 + p_{13}) - \frac{1}{4} (p_4 + 2p_8 + p_{12}) \right\}$$

And

$$\zeta^* (hPa) = \zeta_u^* + \zeta_v^*$$

with

$$\zeta_u^* (hPa) = \frac{\sin \varphi_0}{\sin (\varphi_0 + \Delta \varphi / 2)} \left\{ \frac{1}{2} [(p_{15} + p_{16}) - (p_8 + p_9)] \right\}$$

$$- \frac{\sin \varphi_0}{\sin (\varphi_0 - \Delta \varphi / 2)} \left\{ \frac{1}{2} [(p_8 + p_9) - (p_1 + p_2)] \right\}$$

$$\zeta_v^* (hPa) = \frac{1}{2 \cos^2 \varphi_0} \left\{ \frac{1}{4} [(p_6 + 2p_{10} + p_{14}) - (p_5 + 2p_9 + p_{13})] \right.$$

$$\left. - \frac{1}{4} [(p_4 + 2p_8 + p_{12}) - (p_3 + 2p_7 + p_{11})] \right\}$$

where  $\varphi_0$  is the latitude of the respective central point of the respective grid (55°N, 5°E for the North Sea; 60°N, 20°E for the Baltic Sea), and  $\Delta \varphi$  is 10°. The Baltic Sea grid has been shifted 5° north- and 15° eastwards from the North Sea grid to accommodate for the Coriolis frequency, i.e., to ensure that gales are identified at an identical geostrophic wind and vorticity scale in either region.

The geostrophic wind is a good approximation of the large-scale wind conditions in the free atmosphere. The LWTs are derived from the relationships between the geostrophic wind components and the vorticity. While the classification procedure originally allowed for 27 different weather types, a condensed version is used here that identifies six characteristic weather types in order to assure more reliable and robust statistics. This is achieved by reclassifying the hybrid weather types which appear only five to six times a year, and by evenly distributing the rather undistinctive types into two rotational and four directional types (Löwe, 2009; Löwe et al.,

TABLE 2 Reduced LAMB Weather Type classification criteria based on geostrophic wind ( $V^*$ ), vorticity ( $\zeta^*$ ) and geostrophic wind direction (vdir).

condition	flow	LWT
$ \zeta^*  \leq V^* \sqrt{2}$	directional	NW (if vdir >270) NE (if vdir >0 and vdir ≤90) SE (if vdir >90 and vdir ≤180) SW (if vdir >180 and vdir ≤270)
$ \zeta^*  > V^* \sqrt{2}$	rotational	C (if $\zeta^* \geq 0$ ) A (if $\zeta^* < 0$ )

2013). These six characteristic weather types are anticyclonic (A), cyclonic (C), north-east (NE), north-west (NW), south-east (SE), and south-west (SW). Although technically only valid at its respective central points, the results are representative of the North- and Baltic Seas.

LWT A is an anticyclone centered over the area with its core at or near the central point and is characterized by mainly dry conditions and light winds, warm in the summer season and cold in winter due to the influence of the continental land masses. LWT C in contrast is a cyclone or depression centered over the area, usually wet with variable wind conditions, mild temperatures in autumn and winter and colder temperatures in spring and summer, oftentimes accompanied by gales or thunderstorms.

The directional LWTs (NE, SE, SW, NW) are defined due to the quadrant, i.e., the directional boundaries of a four-point compass (0°, 90°, 180°, 270°). The classification criteria are summarized in Table 2. LWT SW is characterized by low pressure systems traveling the Atlantic eastwards with mild temperatures, rainfall and frequent gales during the winter months and cool conditions in summer. LWT NW is accompanied by cooler conditions than SW but shows similar overall conditions with low-pressure systems traveling eastwards from Island into the North Sea with greatest intensity over the Baltic or Scandinavia and gale strength winds (Lamb, 1950). Westerly winds would also push water masses onshore the German North Sea Coast and offshore the coast of Schleswig-Holstein, where Kiel and Flensburg are located. LWT NE brings cold arctic air to the area, resulting e.g., in severe frost in winter and water pushed onshore the German Baltic Sea Coast. LWT SE is the main driver for negative storm surges in the German Bight of the North Sea and is characterized by a positive pressure anomaly over Scandinavia and a negative pressure anomaly over the north Atlantic and the Iberian Peninsula (Jensen et al., 2022).

## 2.2.3 Gale strength

Another variable that is relevant for storm surges and provided by the LWT classification is the gale strength. A gale index  $G^*$  is calculated, based on an elliptical relationship between geostrophic wind ( $V^*$ ) and vorticity ( $\zeta^*$ ) (Löwe, 2005, appendix A3, GL. A16):

$$G^* = \sqrt{V^{*2} + \frac{\zeta^{*2}}{4}}$$

As part of the classification, the gale index is then classified as G (“Gale”), SG (“Severe Gale”) and VSG (“Very Severe Gale”) if it

exceeds the 90th, 98th and 99.73rd percentile of the climatological  $G^*$  distribution based on a reference period of 1971–2000 (Löwe, 2009; Löwe et al., 2013). All values below the 90th percentile are associated with NUL (“No Gale”). Both, daily LWTs and gale strengths data for the North and Baltic Seas from 1948 till 2024 are referenced *via* the World Data Center for Climate (WDCC), hosted and maintained by the German Climate Computing Center (DKRZ) in Hamburg, Germany (see Loewe, 2022; Loewe and Schade, 2024).

In the specific case depicted in Figure 2, a severe storm surge (storm “Babet”, UK Met Office) was observed on 20 October 2023, along the German and Danish Baltic Sea coast, caused by easterly winds (LWT = A, Gale = G), as well as a negative storm surge (e.g., Jensen et al., 2022) at the North Sea Coast (LWT = SE, Severe Gale = SG). This event was described in several publications (e.g., Groll et al., 2024; Kiesel et al., 2024) and led to substantial damages like dyke breaks and flooding in several cities, e.g., Flensburg and Schleswig at the Baltic Sea coast of Schleswig-Holstein, Germany.

### 2.2.4 Effective wind

The combination of large-scale wind direction, as indicated by the LWT, and gale strength can be captured by the effective wind. The effective wind is defined as the wind component (or the part of the wind vector) that has the strongest effect on the water level at a specific location. In the cases examined here, this is the wind direction driving the water directly to the gauge station resulting in a storm surge.

In order to identify the wind direction for the effective wind at each station, the respective mean geostrophic wind direction has been calculated by averaging the geostrophic wind components at the respective calendar days of the observed storm surges. In case the peak water levels occurred before 6 a.m., the geostrophic wind components of the previous day were used in order to link the delayed response of the water body to the influence of the wind conditions. Then, the daily geostrophic wind vectors for the entire study period were projected onto the wind direction to calculate the absolute effective wind ( $v_{\text{eff}}$ ), combining both wind direction and strength into a scalar metric for simplified analysis. Note that the effective wind calculated here is specific to storm surges at the respective gauge stations and the observational time period. This approach has been employed in several studies on storm surges - or their opposite, “negative storm surges” - (e.g., Ganske et al., 2018; Jensen et al., 2022; Koziar et al., 2006) and it has been proven to be effective.

## 3 Results

The data catalogues of observed peak water levels (see Section 2.1.1) allow a statistical analysis of the common atmospheric conditions at the time of storm surges. The Lamb classification method is employed as described in Section 2.2 to investigate the LWTs, gale indices and effective winds at the respective calendar days of observed storm surges. To account for the influence of the wind conditions on the respective events, all peak water levels occurring before 6 a.m. are linked to the atmospheric conditions the previous day.

## 3.1 North sea (gauge cuxhaven)

### 3.1.1 Observed storm surge events

Figure 3A shows the distribution of LWT occurrences at Cuxhaven in the German Bight, calculated from daily NCEP/NCAR R1 SLP data for the entire period (1951–2022), while Figure 3B shows the distribution of LWT occurrences specifically for observed storm surges. The two distributions differ noticeably. During storm surges, the occurrence of LWT NW is threefold higher than in the climatological mean, 61% in total. 14.9% of observed storm surges are associated with LWT SW, and the remaining 24.1% with LWT C, which indicates that the center of the storm is located directly over the central North Sea. Easterly LWTs (SE, NE) are completely missing during storm surges, as well as the LWT A, which could be expected, since westerly winds (especially NW) are needed to push water masses in the direction of the German Bight. Furthermore, the sequence of LWTs SW, C and NW is connected with low pressure systems in this region.

Similarly, to Figures 3, 4 shows the distribution of the gale index ( $G^*$ ) derived from the LWT classification. While the probability that a storm (indices G, SG and VSG) occurs is about 9% for all peak water levels, this probability rises to about 84.4% during observed storm surges. The remaining 15.6% show  $G^*$ -values below the 90th percentile, which were therefore classified as no storm. This is the case for 44 storm surge events from the catalogue. In some of those 44 cases, a storm was detected the day before, or the EWL was caused by a combination of untimely tidal high waters and westerly winds not reaching gale strength. In fact, all those 44 EWL cases show persistent westerly conditions in the days and even weeks before the peak high water, and/or high effective geostrophic wind speeds. Therefore, it proves necessary to analyze the directional component together with its strength. Also, at least part of the 44 EWLs classified with “no gale” could be explained by the presence of external surges (Böhme et al., 2023).

For Cuxhaven, the effective wind direction is  $295^\circ$  (Müller-Navarra and Giese, 1999). Figure 5 shows the empirical probability distribution function of the effective wind (Section 2.2.2) as a climatology for the entire period 1951–2022 and during storm surges in [m/s] using the equations from Löwe (2005); appendix A1, GL. A3/A4). The two distributions are clearly different. During storm surges, the effective wind is always positive and mostly higher than 13 m/s which in turn approx. matches the 95th percentile of the climatological distribution that is close to the modal value of 14 m/s. The climatological probability distribution of the effective wind spreads from about  $-23$  m/s to 31 m/s with a mean value of approx. 2.4 m/s, indicating a predominant westerly circulation over the North Sea. It is noticeable that a number of storm surges can be observed at  $v_{\text{eff}}$  values clearly below the extremes of the climatological distribution. This is in sync with below extreme gale values during observed storm surges and shows that the combined effect of a tidal high-water situation and not extreme westerly winds can lead to extreme peak water levels as well. Further, external surges can contribute to the generation of extreme events under non-extreme wind conditions. Nevertheless, the analysis indicates that  $v_{\text{eff}}$  can be used as a proxy to indicate storm surge favorable atmospheric conditions and the 95th percentile of

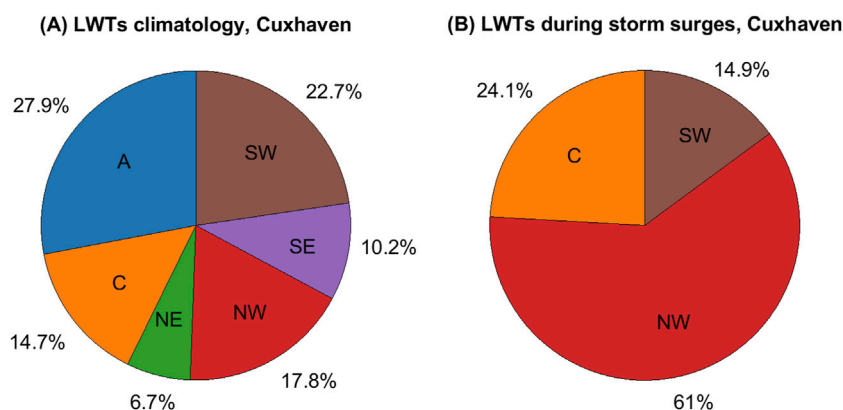


**FIGURE 3**  
Mean distribution of LWTs determined from daily means of NCEP/NCAR R1 sea level pressure (SLP) for the entire period from 1951 to 2022 **(A)** and during observed storm surges at the gauge Cuxhaven between 1951 and 2022 **(B)** Adapted from Schade et al. (2023), Figure 4-1.

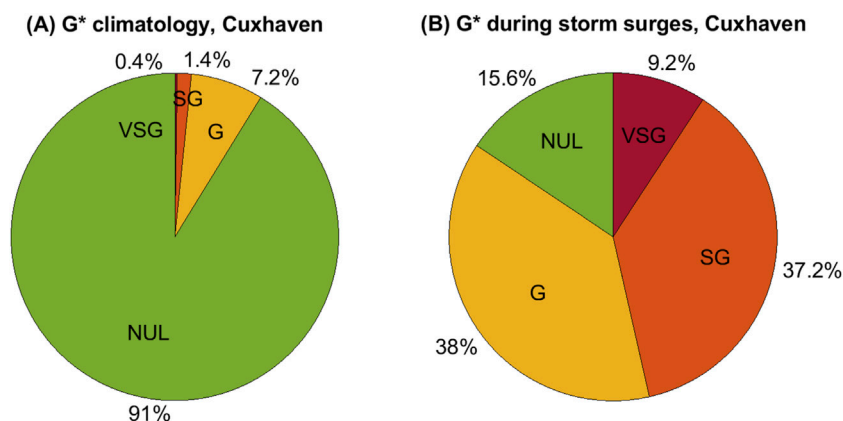


**FIGURE 4**  
Mean distribution of the gale index (G\*) determined from daily means of NCEP/NCAR R1 sea level pressure (SLP) for the entire period from 1951 to 2022 **(A)** and during observed storm surges at the gauge Cuxhaven between 1951 and 2022 **(B)**. Adapted from Schade et al. (2023), Figure 4-2.

the climatological  $v_{eff}$  distribution can serve as a threshold to identify these situations in climate model simulations.

### 3.1.2 Climate change signals using a CMIP6 ensemble

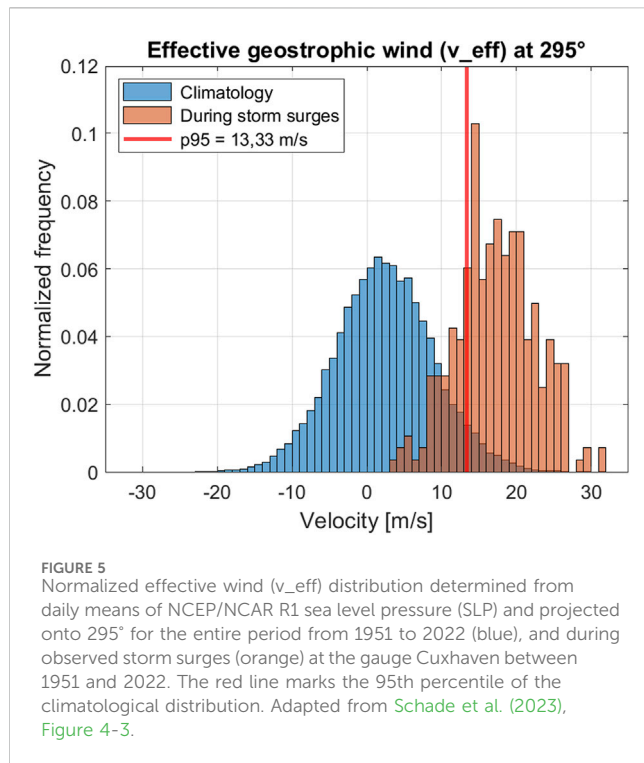
The results from the previous sections demonstrate that both, wind direction and wind speed play a crucial role in triggering storm surges. The question arises whether these conditions might change in the future. In the following we analyze the frequency of westerly LWTs (SW, NW), including LWT C, gale classes, as well as  $v_{eff}$  in four SSP climate scenarios based on the CMIP6 ensemble (Section 2.1.3).

Figure 6A shows the occurrence of the sum of the derived LWTs NW, C, and SW per year for NCEP/NCAR R1, ERA5 and the 23-member CMIP6 ensemble for the historical period (1971–2000) and the far future (2071–2,100) in SSP1-2.6, SSP2-4.5, SSP3-7.0, and SSP5-8.5, respectively. In these plots, two median values are significantly different ( $p < 0.05$ ) if their confidence intervals (marked by the center of the triangular markers) do not

overlap. It can be concluded that the median occurrences of NW, C and SW LWTs in CMIP6 historical is consistent with those in ERA5, while the occurrences of those LWTs calculated from NCEP is lower.

The frequency of relevant LWTs hardly changes with the projected climate change according to the CMIP6 data. In the supplements (Supplementary Figure S1) we show the changes in the frequency for all six LWTs. Here we find that LWT C will occur significantly less in a changing climate. The drop is more pronounced in the higher emission scenario. In contrast, both westerly LWTs (NW,SW) show significant increases. This is arguably due to the projected poleward shift of the storm tracks and the cores of the single storm systems, resulting in a more directly westerly driven circulation and therefore a higher probability in the occurrence of  $v_{eff}$  above the 95th percentile (see Figure 6C).

Figure 6B shows the distribution of the occurrence of gales (G, SG, and VSG) during LWTs SW, C, and NW per year for the historical period and the far future. A significant decrease for the



SSP1-2.6 scenario is apparent, while the higher scenarios reach historical levels, but with an extended range regarding the extremes.

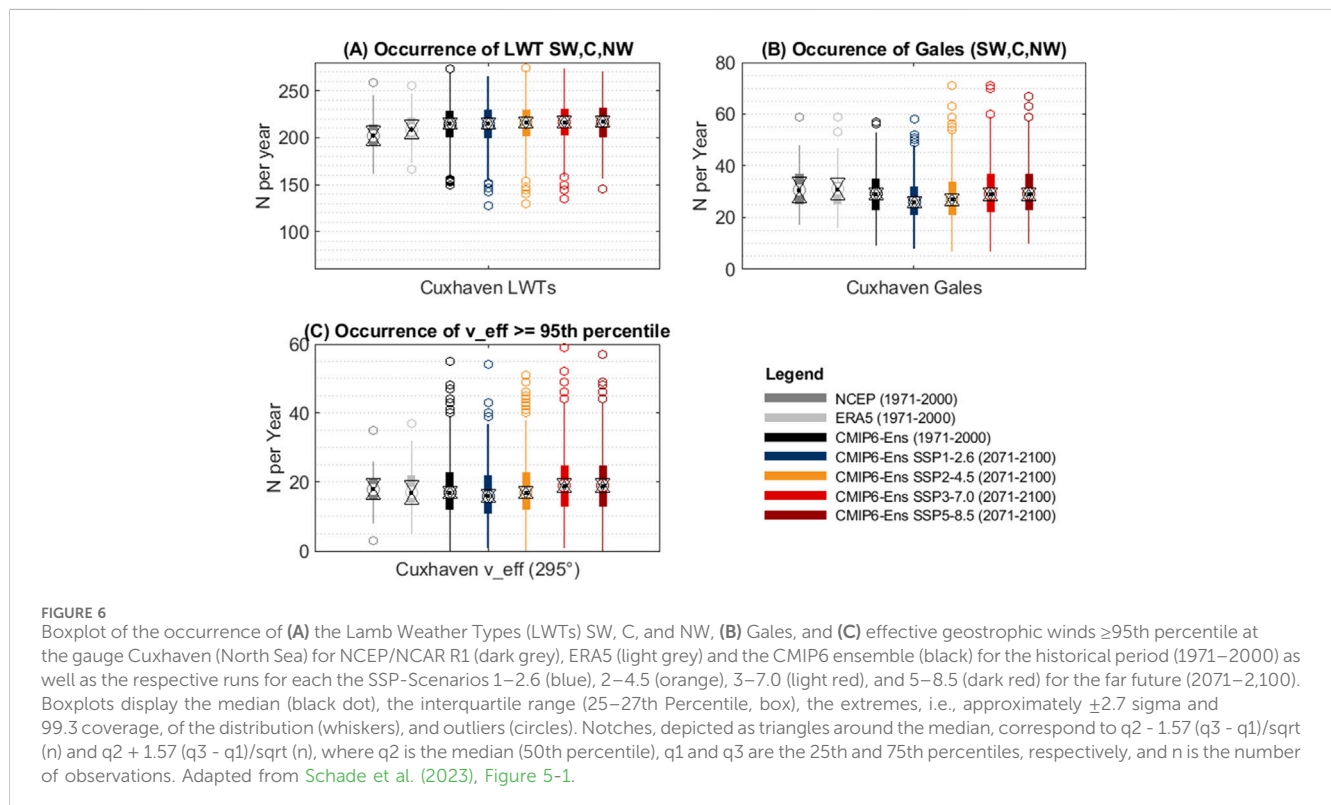
Figure 6C shows the distribution of the occurrence of effective winds being above the 95th percentile of the climatological

probability distribution function of the historical period. For NCEP, this 95th percentile approximately matches the value of 13 m/s, and we have seen in Figure 5 that the majority of storm surges were caused by effective winds beyond this threshold. Hence, we consider such extreme effective winds a reasonable proxy for the risk of storm surges, without including the actual tide phases (or sea level rise for that matter). CMIP6 shows a shift towards more frequent situations with extreme effective winds under the SSP3-7.0, and SSP5-8.5 scenarios. These scenarios have a significantly higher median than in the historical scenario (see also Supplementary Figure S2). This shift can be explained with the significant increase of westerly LWTs, even though the mean frequency of gales during relevant LWT-situations does not change.

## 3.2 Baltic Sea

### 3.2.1 Observed storm surge events

Figure 7 shows the frequency distribution of LWTs for observed storm surges at the Baltic Sea gauge stations in Flensburg (A), Kiel-Holtenau (B), Warnemünde (C), and Koserow (D) between 1951 and 2022. Obviously, the situation in the Baltic Sea is completely different from the North Sea. First of all, the storm surge favorable atmospheric conditions are dominated by easterly winds, especially for the more exposed stations at Koserow and Warnemünde (see Figure 1). But even at those stations, storm surges are recorded when the wind comes from westerly directions, i.e., blowing offshore instead of onshore. This is most pronounced for Kiel-Holtenau and Flensburg.





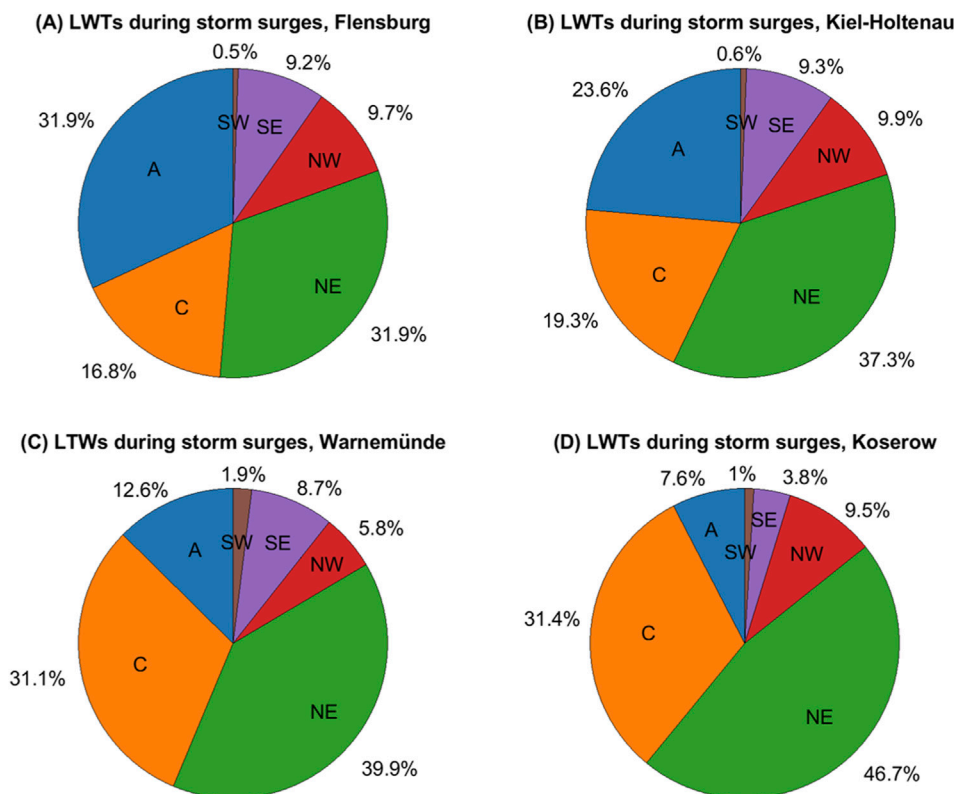


**FIGURE 7**  
Mean distribution of LWTs determined from daily means of NCEP/NCAR R1 sea level pressure (SLP) during observed storm surges at the gauges Flensburg (A) Kiel-Holtenau (B) Warnemünde (C) and Koserow (D) between 1951 and 2022.

Nevertheless, to obtain a  $v_{eff}$  direction to describe the direct atmospheric trigger for the Baltic Sea gauge stations, the mean  $v_{eff}$  has been derived from the distribution during observed storm surges, exemplary shown as wind roses for four Baltic Sea stations (Figure 8). For Koserow (D), the mean  $v_{eff}$  direction is  $34^\circ$ . Compared to the other Baltic Sea stations, the wind rose is narrower around the mean  $v_{eff}$  direction due to its more exposed location, but still shows some westerly winds during storm surge events. Kiel-Holtenau (B), and Flensburg (A), especially, show a wide spread in directions from north-west to south-east, yet, most directions are north-easterly during storm surges. Therefore, the mean  $v_{eff}$  direction seems mostly feasible to assess the direct atmospheric circulation influence and changes thereof in future scenarios.

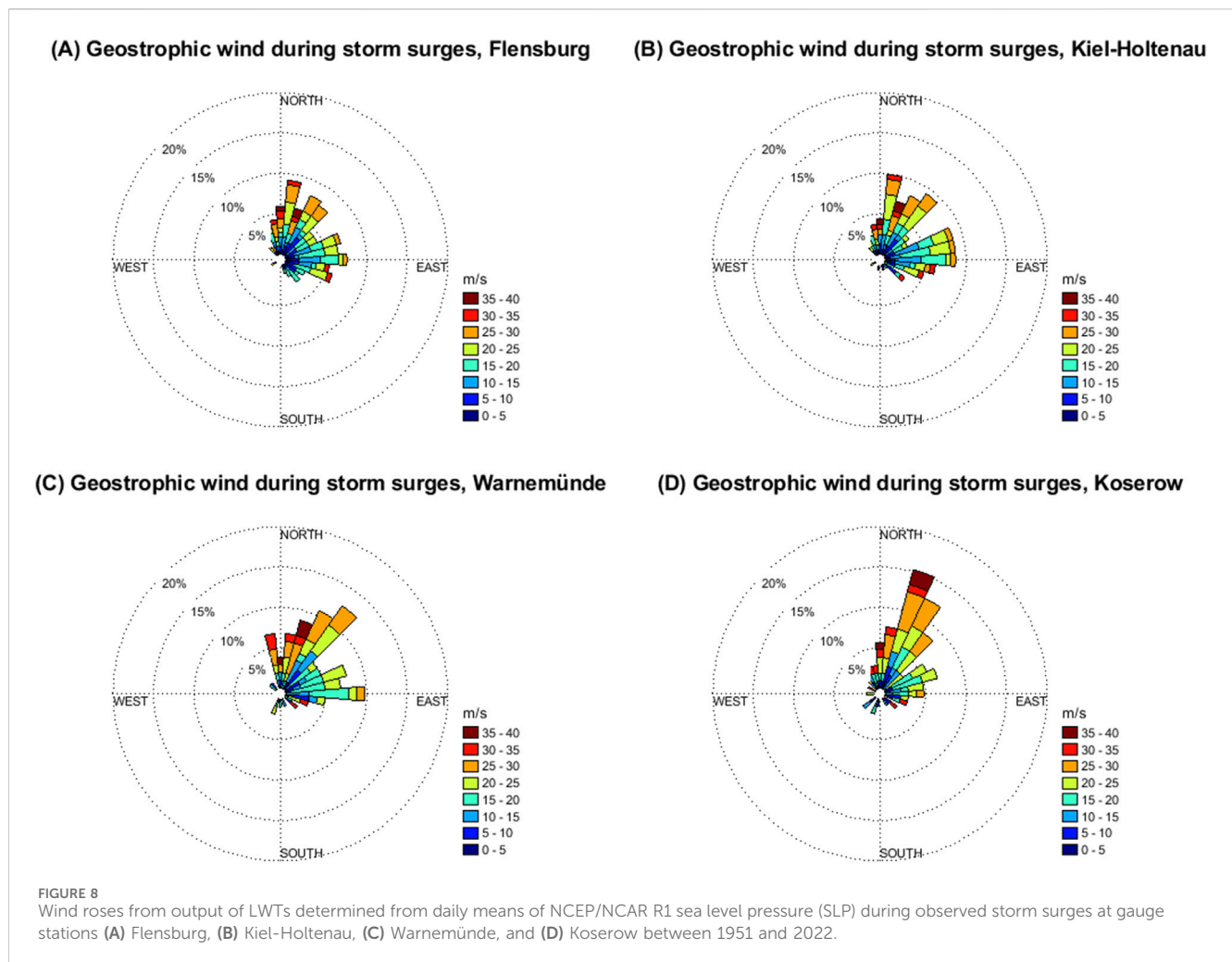
Figure 9 shows the empirical probability distribution function of the effective wind speeds for the entire period 1951–2022 and during storm surges for the Baltic Sea stations. As in Cuxhaven, a clear distinction between the two distributions is obvious, but here these differences are not as pronounced. The main difference, however, is that a number of storm surges can be observed at negative  $v_{eff}$  values. This shows again that the atmospheric component is not the sole driver of these extreme peak water level events which becomes even more obvious at the stations Kiel-Holtenau (B) and Flensburg (A) where the 95th percentile is not including the modal value of the geostrophic effective wind speed.

However, the analysis indicates that the 95th percentile of the climatological  $v_{eff}$  distribution can serve as threshold to identify

storm surge favorable atmospheric conditions in climate model simulations as well. It has to be pointed out here that the 90th percentile could be used instead, especially for the stations Kiel-Holtenau (B) and Flensburg (A), since the modal value of the distribution for actual storm surge events would be included then as well. For consistency reasons, we display the results for the 95th percentile here, but the results using the 90th percentile are included in the supplements. While the total values change of course, the tendencies of the climate change projections do not differ from those using the 95th percentile. We will present the results for Koserow in the following, since the exposed location of the station makes it the best exemplary study case based on the previous results. The results for the other stations will be discussed, but the respective figures are placed in the supplements.

### 3.2.2 Climate change signals using the CMIP6 ensemble

Figure 10A shows the distribution of the occurrence of the relevant LWTs NE and C per year for NCEP/NCAR R1, ERA5 and the 23-member CMIP6 ensemble for Koserow for the historical period (1971–2000) and the far future (2071–2,100) in SSP1-2.6, SSP2-4.5, SSP3-7.0, and SSP5-8.5, respectively. As for Cuxhaven, the CMIP6 historical ensemble is consistent with ERA5 values regarding the median frequency for the relevant LWTs. The frequency of relevant LWTs hardly changes in the future regardless of the scenario. The same holds true for the other stations (see supplements). Easterly LWTs that favor storm surge conditions



in the Baltic occur much less frequent than the corresponding westerly LWTs in Cuxhaven. It should be mentioned that southerly LWTs (SE, SW) are not well represented with the CMIP6 ensemble compared to both reanalyses (Supplementary Figure S3): While SW is significantly underestimated, SE is significantly overestimated. Yet, both LWTs are seldomly associated with storm surges in the Baltic Sea (see Figure 7).

Figure 10B shows the distribution of the occurrence of gales (G, SG, and VSG) during LWTs NE, and C per year for the historical period and the far future. A significant decrease for all the SSP scenarios is apparent, while not as strong for the scenario SSP3-7.0 (see Supplementary Figure S4 for a depiction of changes in the medians and confidence intervals only). An overall decrease can be seen for all scenarios at all the Baltic Seas stations (see Supplementary Figures S5-S7). Compared to gales from westerly directions in the North Sea, easterly gales in the Baltic Sea in general are considerably less frequent as well.

Figure 10C shows the distribution of the occurrence of effective winds being above the 95th percentile of the climatological probability distribution function of the historical period. The CMIP6 data shows a shift towards significant less frequent situations with extreme effective winds under the SSP3-7.0, and SSP5-8.5 scenarios regarding the median frequency. This cannot be

explained with the changes of the relevant LWTs NE and C (see Supplementary Figure S3): While there is a decrease of LWT NE for the scenarios SSP3-7.0 and SSP5-8.5, an increase of LWT C for the respective scenarios and SSP2-4.5 can be seen. It is therefore likely explained by the decrease in easterly gales as mentioned above.

Using the 90th percentile of the climatological  $v_{eff}$  distribution as threshold, the results do not change except of course for the overall mean values increasing and, likewise, the amount of decrease in the far future (see Supplementary Figures S8-S11), i.e., the situations with extreme effective winds decrease even more. But one could argue that “extremes” described with values above the 90th percentile of a distribution are not considered statistically extreme values anymore.

## 4 Discussion

Our investigations of LWTs over the North Sea show that westerly and cyclonic LWTs are the atmospheric drivers at days with observed storm surges at Cuxhaven. For the Baltic Sea region, storm surges can occur with each weather type. Yet, favorable LWTs at the stations Koserow and Warnemünde are NE and C with the addition of A for Kiel and Flensburg.

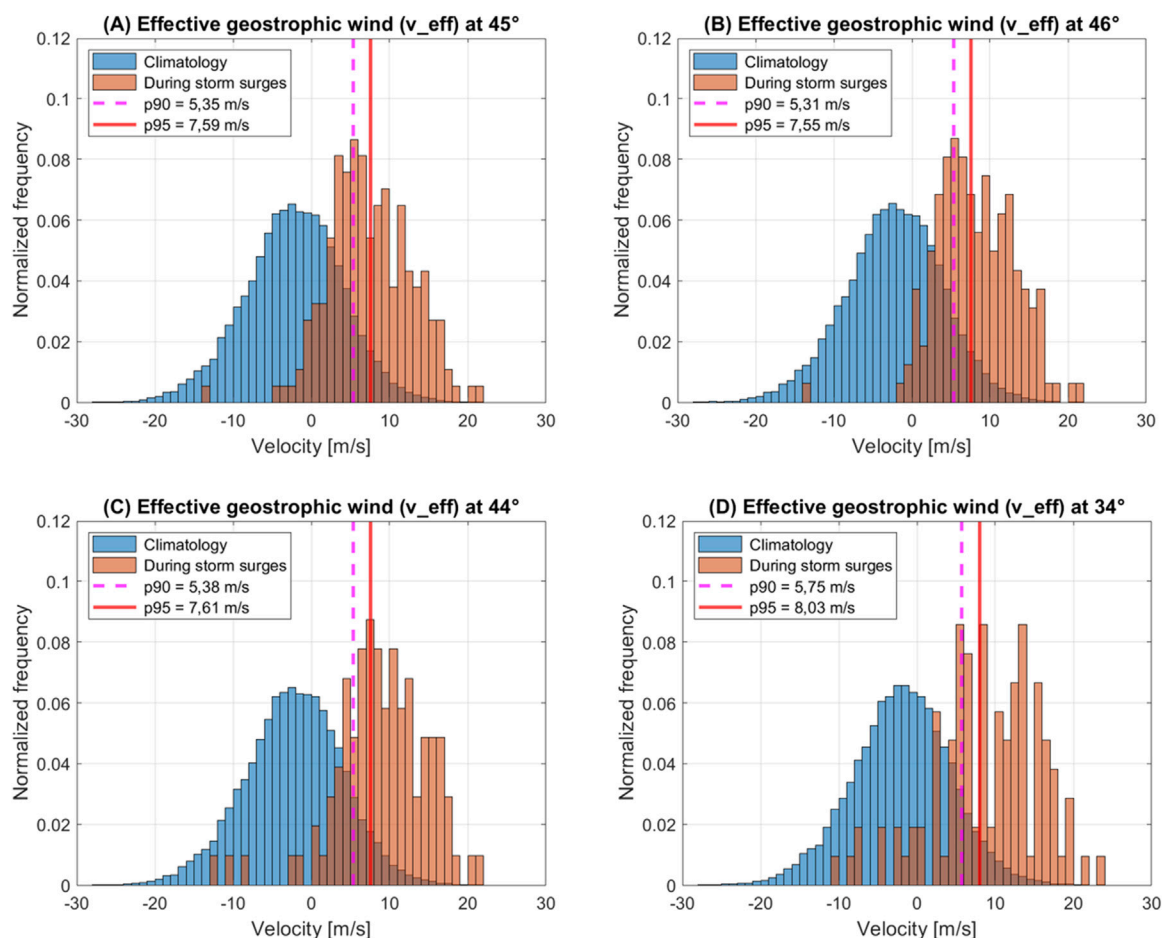


FIGURE 9

Normalized effective wind ( $v_{\text{eff}}$ ) distributions determined from daily means of NCEP/NCAR R1 sea level pressure (SLP) for the entire period from 1951 to 2022 (blue), and during observed storm surges (orange) at the gauges (A) Flensburg, (B) Kiel-Holtenau, (C) Warnemünde, and (D) Koserow between 1951 and 2022. The red lines mark the 95th percentiles of the climatological distributions, the dashed magenta lines the 90th percentiles.

Towards the end of the 21st century (2071–2,100), the multi-model ensemble projects a significant increase in the frequency of atmospheric conditions favouring storm surges, i.e., westerly effective geostrophic winds, in the direction of Cuxhaven under the scenarios SSP3-7.0 and SSP5-8.5. In contrast, a significant decrease of easterly effective geostrophic winds can be seen in the direction of all four locations at the Baltic Sea coast. These results are in accordance with the projected increased frequency under westerly directions and a north-western shift of the storm tracks in climate projections over the North and Baltic Seas region described by other investigations (e.g., Donat et al., 2010; Heinrich et al., 2024; Plavcová and Kysely, 2013).

Further, our study supports similar investigations that a direct atmospheric trigger is not the sole contributor for the development of EWLs in the German Baltic Sea, and that other factors like the pre-filling due to westerly winds, pushing water masses from the North Sea through the Skagerrak (the strait running between the Jutland peninsula of Denmark, the east coast of Norway, and the west coast of Sweden) or the seiche-effect have to be considered. Groll et al. (2024) for example, showed that two out of the recent three mayor Baltic Sea storm surges were caused by a combination of wind-induced water level and prefilling rather than by extremes in

direct atmospheric effects alone. In addition, Lorenz et al. (2024) found that from the three main influences for EWLs (storm surges, seiches, and pre-filling), storm surges dominate the western parts of the Baltic Sea while in the Central and Northern Baltic Sea pre-filling is the main influence (see e.g., their Figure 3). We therefore conclude that EWLs at more exposed stations at the German Baltic Sea coast like Koserow - that are more receptive to a direct wind influence - can be described using our approach while it still works reasonably well for the stations Warnemünde, Kiel-Holtenau and Flensburg.

In the North Sea area, LWTs have been tested as part of the European Cooperation in Science and Technology (COST) Action 733 “Harmonisation and Applications of Weather Type Classifications for European regions” (Philipp et al., 2010), and have proven useful in climate studies (e.g., Fealy and Mills, 2018; Jensen et al., 2022). Recent studies by Krieger and Weisse (2025) using a similar approach namely, calculating geostrophic wind speeds from a triangle of SLP grid points located over the German Bight derived from a slightly enhanced CMIP6 ensemble support our findings of increased (north) westerly winds and a decrease in easterly winds. They also found increases in the very high percentiles (above the 99th), i.e., effective wind speeds above 30 m/s (their Figures 9, 10) in the German Bight. They concluded that the

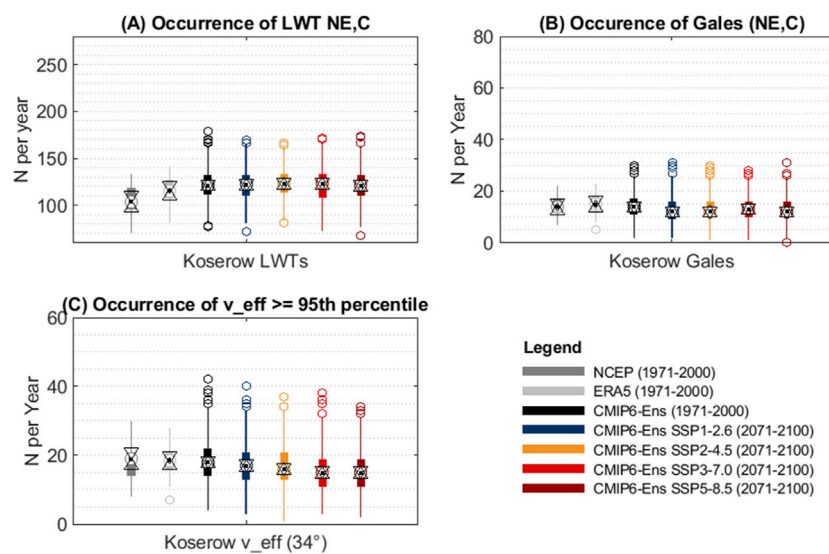


FIGURE 10

Boxplot of the occurrence of (A) the Lamb Weather Types (LWTs) NE, and C, (B) Gales, and (C) effective geostrophic winds  $\geq 95$ th percentile at the gauge Koserow (Baltic Sea) for NCEP/NCAR R1 (dark grey), ERA5 (light grey) and the CMIP6 ensemble (black) for the historical period (1971–2000) as well as the respective runs for each the SSP-Scenarios 1–2.6 (blue), 2–4.5 (orange), 3–7.0 (light red), and 5–8.5 (dark red) for the far future (2071–2100). Boxplots display the median (black dot), the interquartile range (25–75th Percentile, box), the extremes, i.e., approximately  $\pm 2.7$  sigma and 99.3 coverage, of the distribution (whiskers), and outliers (circles). Notches, depicted as triangles around the median, correspond to  $q2 - 1.57(q3 - q1)/\sqrt{n}$  and  $q2 + 1.57(q3 - q1)/\sqrt{n}$ , where  $q2$  is the median (50th percentile),  $q1$  and  $q3$  are the 25th and 75th percentiles, respectively, and  $n$  is the number of observations.

likelihood of very severe storms may increase significantly in a warming climate despite an overall reduction of storm activity. This was also found by Priestley et al., 2020 and is in line with projected storm track changes described by Harvey et al. (2020).

To conclude, we want to highlight that our method can be applied easily to global as well as regional climate model simulations which makes it an effective tool for climate change investigations of the atmospheric conditions that may trigger EWLs. We argue and show that the (large) majority of storm surges are associated with the respective atmospheric circulation patterns. Analysis of the frequency of these weather types therefore yields results that are valuable with respect to potential changes in storm surge risk. Furthermore, a robust assessment of potential climate change signals requires the analysis of multi-model ensembles. These are still only available from GCMs which unfortunately provide only limited output. Therefore, any methods based solely on GCMs without having sub daily information is of particular interest for the community. Further, an advantage of this method is the independence of geostrophic wind speeds on surface wind parametrizations which may differ between models and introduce biases in the analysis of absolute surface or near-surface wind speeds and derived trends (see Krieger and Weisse, 2025). More in depth analyses on storm tracks, however, require a different approach (e.g., Schaffer et al., 2024; Schaffer et al., 2023).

It should be noted here as well that the virtually certain climate change signal of the sea level rise has to be added when assessing the full risk of EWLs along the coastlines in the future. Also, compound events with more than one contributor to add to the EWLs have to be considered. In these cases, the single contributors do not have to be extreme *per se*, but the combination of two or more contributors may lead to a resulting EWL. This holds especially true for the Baltic

Sea, where pre-filling, seiches, sea level rise, and direct atmospheric triggers have to be considered.

## Data availability statement

Existing datasets are available from the following publicly accessible sources: 1) Water level observations at Cuxhaven, Kiel-Holtenau, Flensburg, Warnemünde, and Koserow are available from the Federal Waterways and Shipping Administration (WSV). 2) NCEP/NCAR SLP data are operationally used at BSH for calculations of Lamb Weather Types and Gales (see <https://www.wdc-climate.de/ui/project?acronym=BSHwt>) and are obtained via the NOAA/OAR/ESRL Physical Sciences Laboratory, Boulder, Colorado, USA. (2014). NCEP/NCAR Reanalysis 1: Surface - Sea Level Pressure (Daily), 1948-continuing. <https://www.psl.noaa.gov/data/gridded/data.ncep.reanalysis.surface.html>. 3) The ERA5-SLP data is publicly available from the Copernicus Climate Change Service (C3S) Climate Data Store (CDS, <https://cds.climate.copernicus.eu/datasets>). Hersbach, H., Bell, B., Berrisford, P., Biavati, G., Horányi, A., Muñoz Sabater, J., Nicolas, J., Peubey, C., Radu, R., Rozum, I., Schepers, D., Simmons, A., Soci, C., Dee, D., Thépaut, J.-N. (2018): ERA5 hourly data on single levels from 1979 to present. Copernicus Climate Change Service (C3S) Climate Data Store (CDS). (accessed on 13 June 2022), DOI: 10.24381/cds.adbb2d47; 4) CMIP6 SLP data: The SLP-fields are publicly available from the from the Earth System Grid Federations (ESGF) for the respective experiments: 5) CMCC-CM2-SR5 (2020): Lovato, Tomas; Peano, Daniele (2020). CMCC CMCC-CM2-SR5 model output prepared for CMIP6 ScenarioMIP. Version 20220627. Earth System Grid Federation. <https://doi.org/10.22033/ESGF/CMIP6.1365>.



6) CNRM-CM6-1-HR (2019): Voldoire, Aurore (2019). CNRM-CERFACS CNRM-CM6-1-HR model output prepared for CMIP6 ScenarioMIP. Version 20220617. Earth System Grid Federation. <https://doi.org/10.22033/ESGF/CMIP6.1388>. 7) EC-Earth3 (2019): EC-Earth Consortium (EC-Earth) (2019). EC-Earth-Consortium EC-Earth3 model output prepared for CMIP6 ScenarioMIP. Version 20220603. Earth System Grid Federation. <https://doi.org/10.22033/ESGF/CMIP6.251>. 8) IPSL-CM6A-LR (2019): Boucher, Olivier; Denvil, Sébastien; Levvasseur, Guillaume; Cozic, Anne; Caubel, Arnaud; Foujols, Marie-Alice; Meurdesoif, Yann; Cadule, Patricia; Devilliers, Marion; Dupont, Elliott; Lurton, Thibaut (2019). IPSL IPSL-CM6A-LR model output prepared for CMIP6 ScenarioMIP. Version 20220603. Earth System Grid Federation. <https://doi.org/10.22033/ESGF/CMIP6.1532>. 9) MIROC6 (2019): Shiogama, Hideo; Abe, Manabu; Tatebe, Hiroaki (2019). MIROC MIROC6 model output prepared for CMIP6 ScenarioMIP. Version 20220610. Earth System Grid Federation. <https://doi.org/10.22033/ESGF/CMIP6.898>. 10) MPI-ESM1-2-LR (2019): Wieners, Karl-Hermann; Giorgetta, Marco; Jungclaus, Johann; Reick, Christian; Esch, Monika; Bittner, Matthias; Gayler, Veronika; Haak, Helmuth; de Vrese, Philipp; Raddatz, Thomas; Mauritsen, Thorsten; von Storch, Jin-Song; Behrens, Jörg; Brovkin, Victor; Claussen, Martin; Crueger, Traute; Fast, Irina; Fiedler, Stephanie; Hagemann, Stefan; Hohenegger, Cathy; Jahns, Thomas; Kloster, Silvia; Kinne, Stefan; Lasslop, Gitta; Kornbluh, Luis; Marotzke, Jochem; Matei, Daniela; Meraner, Katharina; Mikolajewicz, Uwe; Modali, Kameswarrao; Müller, Wolfgang; Nabel, Julia; Notz, Dirk; Peters-von Gehlen, Karsten; Pincus, Robert; Pohlmann, Holger; Pongratz, Julia; Rast, Sebastian; Schmidt, Hauke; Schnur, Reiner; Schulzweida, Uwe; Six, Katharina; Stevens, Bjorn; Voigt, Aiko; Roeckner, Erich (2019). MPI-M MPIESM1.2-LR model out-put prepared for CMIP6 ScenarioMIP. Version 20220616. Earth System Grid Federation. <https://doi.org/10.22033/ESGF/CMIP6.793>. 11) MRI-ESM2-0 (2019): Yukimoto, Seiji; Koshiro, Tsuyoshi; Kawai, Hideaki; Oshima, Naga; Yoshida, Kohei; Urakawa, Shogo; Tsujino, Hiroyuki; Deushi, Makoto; Tanaka, Taichu; Hosaka, Masahiro; Yoshimura, Hiromasa; Shindo, Eiki; Mizuta, Ryo; Ishii, Masayoshi; Obata, Atsushi; Adachi, Yukimasa (2019). MRI MRI-ESM2.0 model output prepared for CMIP6 ScenarioMIP. Version 20220807. Earth System Grid Federation. <https://doi.org/10.22033/ESGF/CMIP6.638>.

## Author contributions

NS: Writing – review and editing, Methodology, Writing – original draft, Conceptualization, Investigation, Visualization, Validation. CJ: Writing – original draft, Investigation, Methodology, Writing – review and editing. TK: Supervision, Conceptualization, Writing – review and editing, Investigation, Writing – original draft.

## References

Bell, B., Hersbach, H., Simmons, A., Berrisford, P., Dahlgren, P., Horányi, A., et al. (2021). The ERA5 global reanalysis: preliminary extension to 1950. *Quart. J. R. Meteorol. Soc.* 147, 4186–4227. doi:10.1002/qj.4174

## Funding

The author(s) declare that financial support was received for the research and/or publication of this article. This research is part of the Research Network funded by the German Federal Ministry of Transport (BMV).

## Acknowledgments

Baltic Sea peak water levels have been provided by Ines Perlet-Markus and Jürgen Holfort of the German Federal Maritime and Hydrographic Agency (BSH). We acknowledge the World Climate Research Programme (WCRP) for coordinating and promoting CMIP6. We thank the climate modeling groups for producing and making available their model output, the Earth System Grid Federation (ESGF) for archiving the data and providing access, and the multiple funding agencies who support CMIP6 and ESGF. We thank the German Climate Computing Center (DKRZ) for providing their computing resources, as well as Claudia Hinrichs and Laura Schaffer for additional review and proof-reading.

## Conflict of interest

The authors declare that the research was conducted in the absence of any commercial or financial relationships that could be construed as a potential conflict of interest.

## Generative AI statement

The author(s) declare that no Generative AI was used in the creation of this manuscript.

## Publisher's note

All claims expressed in this article are solely those of the authors and do not necessarily represent those of their affiliated organizations, or those of the publisher, the editors and the reviewers. Any product that may be evaluated in this article, or claim that may be made by its manufacturer, is not guaranteed or endorsed by the publisher.

## Supplementary material

The Supplementary Material for this article can be found online at: <https://www.frontiersin.org/articles/10.3389/fenvs.2025.1601836/full#supplementary-material>

Böhme, A., Gerkensmeier, B., Bratz, B., Krautwald, C., Müller, O., Goseberg, N., et al. (2023). Improvements to the detection and analysis of external surges in the north sea. *Nat. Hazards Earth Syst. Sci.* 23, 1947–1966. doi:10.5194/nhess-23-1947-2023

- Bott, F., Lohrengel, A.-F., Forbriger, M., Ganske, A., Haller, M., and Herrmann, C. (2020). Klimawirkungsanalyse des Bundesverkehrssystems im Kontext von Stürmen - Schlussbericht des Schwerpunktthemas Sturmgefahren (SP-104) im Themenfeld 1 des BMVI-Expertenetzwerks. doi:10.5675/ExpNBF2020.2020.05
- Boucher, O., Servonnat, J., Albright, A. L., Aumont, O., Balkanski, Y., Bastrikov, V., et al. (2020). Presentation and evaluation of the IPSL-CM6A-LR climate model. *J. Adv. Model Earth Syst.* 12, e2019MS002010. doi:10.1029/2019MS002010
- Brands, S. (2022). A circulation-based performance atlas of the CMIP5 and 6 models for regional climate studies in the northern hemisphere mid-to-high latitudes. *Geosci. Model Dev.* 15, 1375–1411. doi:10.5194/gmd-15-1375-2022
- Bundesamt für Seeschifffahrt (2025). Storm surges. Available online at: [https://www.bsh.de/EN/TOPICS/Water\\_levels\\_and\\_tides/Storm\\_surges/Storm\\_surges\\_node.html](https://www.bsh.de/EN/TOPICS/Water_levels_and_tides/Storm_surges/Storm_surges_node.html) (Accessed June 24, 25).
- Buthe, B., Jakubowski, D. P., and Pütz, T., (2015). BBSR-analysen KOMPAKT 06/2015.
- Cherchi, A., Fogli, P. G., Lovato, T., Peano, D., Iovino, D., Gualdi, S., et al. (2018). Global mean climate and main patterns of variability in the CMCC-CM2 coupled model. *J. Adv. Model Earth Syst.* 2018MS001369. 11, 185–209. doi:10.1029/2018MS001369
- Demuzere, M., Werner, M., van Lipzig, N. P. M., and Roeckner, E. (2009). An analysis of present and future ECHAM5 pressure fields using a classification of circulation patterns. *Int. J. Climatol.* 29, 1796–1810. doi:10.1002/joc.1821
- Donat, M., Leckebusch, G., Pinto, J., and Ulbrich, U. (2010). European storminess and associated circulation weather types: future changes deduced from a multi-model ensemble of GCM simulations. *Clim. Res.* 42, 27–43. doi:10.3354/cr00853
- Döscher, R., Acosta, M., Alessandri, A., Anthoni, P., Arsouze, T., Bergman, T., et al. (2022). The EC-Earth3 Earth system model for the coupled model intercomparison project 6. *Geosci. Model Dev.* 15, 2973–3020. doi:10.5194/gmd-15-2973-2022
- Eyring, V., Bony, S., Meehl, G. A., Senior, C. A., Stevens, B., Stouffer, R. J., et al. (2016). Overview of the coupled model intercomparison project phase 6 (CMIP6) experimental design and organization. *Geosci. Model Dev.* 9, 1937–1958. doi:10.5194/gmd-9-1937-2016
- Fealy, R., and Mills, G. (2018). Deriving lamb weather types suited to regional climate studies: a case study on the synoptic origins of precipitation over Ireland. *Int. J. Climatol.* 38, 3439–3448. doi:10.1002/joc.5495
- Fernandez-Granja, J. A., Casanueva, A., Bedia, J., and Fernandez, J. (2021). Improved atmospheric circulation over Europe by the new generation of CMIP6 Earth system models. *Clim. Dyn.* 56, 3527–3540. doi:10.1007/s00382-021-05652-9
- Ganske, A., Fery, N., Gaslikova, L., Grabemann, I., Weisse, R., and Tinz, B. (2018). Identification of extreme storm surges with high-impact potential along the German north sea coastline. *Ocean. Dyn.* 68, 1371–1382. doi:10.1007/s10236-018-1190-4
- Groll, N., Gaslikova, L., and Weisse, R. (2024). Recent Baltic sea storm surge events from a climate perspective (preprint). *Sea. Ocean Coast. Hazards*. doi:10.5194/egusphere-2024-2664
- Harvey, B. J., Cook, P., Shaffrey, L. C., and Schiemann, R. (2020). The response of the northern hemisphere storm tracks and jet streams to climate change in the CMIP3, CMIP5, and CMIP6 climate models. *J. Geophys. Res. Atmos.* 125. doi:10.1029/2020JD032701
- Heinrich, P., Hagemann, S., and Weisse, R. (2024). Automated classification of atmospheric circulation types for compound flood risk assessment: CMIP6 model analysis utilising a deep learning ensemble (preprint). *Review*. doi:10.21203/rs.3.rs-4017900/v1
- Herrera-Lormendez, P., Mastrantonas, N., Douville, H., Hoy, A., and Matschullat, J. (2022). Synoptic circulation changes over central Europe from 1900 to 2100: reanalyses and coupled model intercomparison project phase 6. *Int. J. Climatol.* 42, 4062–4077. doi:10.1002/joc.7481
- Hersbach, H., Bell, B., Berrisford, P., Hirahara, S., Horányi, A., Muñoz-Sabater, J., et al. (2020). The ERA5 global reanalysis. *Q. J. R. Meteorol. Soc.* 146, 1999–2049. doi:10.1002/qj.3803
- Hess, P., and Brezowsky, H. (1952). *Katalog der Großwetterlagen Europas (No. 33), Berichte des Deutschen Wetterdienstes*. Deutscher Wetterdienst. Available online at: <https://dwdbib.dwd.de/retrosammlung/content/titleinfo/4180>.
- Jenkinson, A., and Collison, F. (1977). An initial climatology of gales over the north sea. *Synop. Climatol. branch Memo*. 62, 18.
- Jensen, C., Mahavadi, T., Schade, N. H., Hache, I., and Kruschke, T. (2022). Negative storm surges in the elbe Estuary—large-scale meteorological conditions and future climate change. *Atmosphere* 13, 1634. doi:10.3390/atmos13101634
- Kalnay, E., Kanamitsu, M., Kistler, R., Collins, W., Deaven, D., Gandin, L., et al. (1996). The NCEP/NCAR 40-Year reanalysis project. *Bull. Am. Meteorological Soc.* 77, 437–471. doi:10.1175/1520-0477(1996)077<0437:TNYRP>2.0.CO;2
- Kew, S. F., Selten, F. M., Lenderink, G., and Hazeleger, W. (2013). The simultaneous occurrence of surge and discharge extremes for the rhine Delta. *Nat. Hazards Earth Syst. Sci.* 13, 2017–2029. doi:10.5194/nhess-13-2017-2013
- Kiesel, J., Wolff, C., and Lorenz, M. (2024). Brief communication: from modelling to reality – flood modelling gaps highlighted by a recent severe storm surge event along the German Baltic sea Coast. *Nat. Hazards Earth Syst. Sci.* 24, 3841–3849. doi:10.5194/nhess-24-3841-2024
- Koziar, C., Renner, V., and Wetterdienst, D. (2006). *KFKI-Projekt: muse*. Hamburg: Deutscher Wetterdienst.
- Krieger, D., and Weisse, R. (2025). “CMIP6 multi-model assessment of northeast Atlantic and German bight storm activity (preprint),” in *Natural hazards and extreme Events/human/earth system Interactions/earth system and climate modeling*. doi:10.5194/egusphere-2025-111
- Lamb, H. H. (1950). Types and spells of weather around the year in the British isles: annual trends, seasonal structure of the year, singularities. *Q. J. R. Meteorological Soc.* 76, 393–429. doi:10.1002/qj.49707633005
- Loewe, P. (2022). Lamb weather types (reduced set) and gale days over the north sea since 1948 based on NCEP/NCAR reanalysis 1 daily mean sea level pressure fields. doi:10.26050/WDCC/LambWTyRSetAndGaleDaysOverTheNo
- Loewe, P., and Schade, N. (2024). Lamb weather types (reduced set) and gale days over the Baltic sea since 1948 based on NCEP/NCAR reanalysis 1 daily mean sea level pressure fields. doi:10.26050/WDCC/LambWTyRSetAndGaleDaysOverTheBa
- Lorenz, M., Viigand, K., and Gräwe, U. (2024). Untangling the waves: decomposing extreme sea levels in a non-tidal basin, the Baltic sea (preprint). *Sea. Ocean Coast. Hazards*. doi:10.5194/nhess-2024-198
- Löwe, P. (2005). *Nordseezustand 2003, Berichte des BSH, Nr. 38*, 220p. Available online at: <https://www.bsh.de/download/Berichte-des-BSH-38.pdf>.
- Löwe, P. (2009). *System Nordsee – Zustand 2005 im Kontext langzeitlicher Entwicklungen, Berichte des BSH, Nr. 44, Bundesamt für Seeschifffahrt und Hydrographie, Hamburg und Rostock*. Available online at: <https://www.bsh.de/download/Berichte-des-BSH-44.pdf>.
- Löwe, P., Klein, H., and Weigelt-Krenz, S. (2013). *System Nordsee – 2006 & 2007: Zustand und Entwicklungen, Berichte des BSH, Nr. 49, Bundesamt für Seeschifffahrt und Hydrographie, Hamburg und Rostock*. Available online at: <https://www.bsh.de/download/Berichte-des-BSH-49.pdf>.
- Mauritsen, T., Bader, J., Becker, T., Behrens, J., Bittner, M., Brokopf, R., et al. (2019). Developments in the MPI-M Earth system model version 1.2 (MPI-ESM1.2) and its response to increasing CO<sub>2</sub>. *J. Adv. Model Earth Syst.* 11, 998–1038. doi:10.1029/2018MS001400
- Meyer, E. M. I., and Gaslikova, L. (2024). Investigation of historical severe storms and storm tides in the German bight with century reanalysis data. *Nat. Hazards Earth Syst. Sci.* 24, 481–499. doi:10.5194/nhess-24-481-2024
- Müller-Navarra, S. H., and Giese, H. (1999). Improvements of an empirical model to forecast wind surge in the German bight. *Dtsch. Hydrogr. Z.* 51, 385–405. doi:10.1007/BF02764162
- O'Neill, B. C., Tebaldi, C., van Vuuren, D. P., Eyring, V., Friedlingstein, P., Hurtt, G., et al. (2016). The scenario model intercomparison project (ScenarioMIP) for CMIP6. *Geosci. Model Dev.* 9, 3461–3482. doi:10.5194/gmd-9-3461-2016
- Philipp, A., Bartholy, J., Beck, C., Ericpam, M., Esteban, P., Fettweis, X., et al. (2010). Cost733cat – a database of weather and circulation type classifications. *Phys. Chem. Earth, Parts A/B/C* 35, 360–373. doi:10.1016/j.pce.2009.12.010
- Plavcová, E., and Kyselý, J. (2013). Projected evolution of circulation types and their temperatures over central Europe in climate models. *Theor. Appl. Climatol.* 114, 625–634. doi:10.1007/s00704-013-0874-4
- Priestley, M. D. K., Ackerley, D., Catto, J. L., Hodges, K. I., McDonald, R. E., and Lee, R. W. (2020). An overview of the extratropical storm tracks in CMIP6 historical simulations. *J. Clim.* 33, 6315–6343. doi:10.1175/JCLI-D-19-0928.1
- Riahi, K., van Vuuren, D. P., Kriegler, E., Edmonds, J., O'Neill, B. C., and Fujimori, S. (2017). The Shared Socioeconomic Pathways and their energy, land use, and greenhouse gas emissions implications: An overview. *Global Environmental Change* 42, 153–168. doi:10.1016/j.gloenvcha.2016.05.009
- Riediger, U., and Gratzki, A. (2014). Future weather types and their influence on mean and extreme climate indices for precipitation and temperature in central Europe. *metz* 23, 231–252. doi:10.1127/0941-2948/2014/0519
- Schade, N. H. (2017). Evaluating the atmospheric drivers leading to the December 2014 flood in schleswig-holstein, Germany. *Earth Syst. Dynam.* 8, 405–418. doi:10.5194/esd-8-405-2017
- Schade, N. H., Jensen, C., Schaffer, L., Ditzinger, G. X., Möller, J., and Kruschke, T. (2023). Wirkungsanalyse Sturm/Sturmfluten, Sonderanalysen und methodische Entwicklungen Berichtsreihe des Schwerpunktthemas 101. *Bundesamt für Seeschifffahrt Hydrogr. (BSH)*. doi:10.57802/44q8-4h46
- Schade, N. H., Sadikni, R., Jahnke-Bornemann, A., Hinrichs, I., Gates, L., Tinz, B., et al. (2018). The KLIWAS north sea climatology. Part II: assessment against global reanalyses. *J. Atmos. Ocean. Technol.* 35, 127–145. doi:10.1175/JTECH-D-17-0045.1
- Schaffer, L., Becker, N., Schenk, L., Hinrichs, C., Ditzinger, G., Schade, N. H., et al. (2023). Objective assessment of storm surge risk in the German bight – historical events and future climate change (other). *oral*. doi:10.5194/egusphere-egu23-7236
- Schaffer, L., Boesch, A., Baehr, J., and Kruschke, T. (2024). Development of a wind-based storm surge model for the German bight (preprint). *Sea. Ocean Coast. Hazards*. doi:10.5194/egusphere-2024-3144

- Stryhal, J., and Huth, R. (2019). Trends in winter circulation over the British isles and central Europe in twenty-first century projections by 25 CMIP5 GCMs. *Clim. Dyn.* 52, 1063–1075. doi:10.1007/s00382-018-4178-3
- Tatebe, H., Ogura, T., Nitta, T., Komuro, Y., Ogochi, K., Takemura, T., et al. (2019). Description and basic evaluation of simulated mean state, internal variability, and climate sensitivity in MIROC6. *Geosci. Model Dev.* 12, 2727–2765. doi:10.5194/gmd-12-2727-2019
- Voltaire, A., Saint-Martin, D., S  n  s, S., Decharme, B., Alias, A., Chevallier, M., et al. (2019). Evaluation of CMIP6 DECK experiments with CNRM-CM6-1. *J. Adv. Model. Earth Syst.* 11, 2177–2213. doi:10.1029/2019MS001683
- Wyser, K., Koenigk, T., Fladrich, U., Fuentes-Franco, R., Karami, M. P., and Kruschke, T. (2021). The SMHI large ensemble (SMHI-LENS) with EC-Earth3.3.1. *Model Dev.* 14, 4781–4796. doi:10.5194/gmd-14-4781-2021
- Yukimoto, S., Kawai, H., Koshiro, T., Oshima, N., Yoshida, K., Urakawa, S., et al. (2019). The meteorological research institute Earth system model version 2.0, MRI-ESM2.0: Description and basic evaluation of the physical component. *J. Meteorological Soc. Jpn.* 97, 931–965. doi:10.2151/jmsj.2019-051
- Zappa, G., and Shepherd, T. G. (2017). Storylines of atmospheric circulation change for European regional climate impact assessment. *J. Clim.* 30, 6561–6577. doi:10.1175/JCLI-D-16-0807.1